Application of Solid-Phase Concentration-Dependent HSDM to the Acid Dye Adsorption System

Vinci K. C. Lee, John F. Porter, and Gordon McKay
Dept. of Chemical Engineering, The Hong Kong University of Science and Technology, Clearwater Bay, Kowloon, Hong Kong SAR, China

Alexander P. Mathews
Dept. of Civil Engineering, Kansas State University, Manhattan, KS 66506

DOI 10.1002/aic.10290
Published online in Wiley InterScience (www.interscience.wiley.com).

The fixed-bed adsorption of acid dyes onto granular activated carbon (Chemviron Filtrasorb 400) has been studied using a homogeneous surface diffusion model (HSDM). The model incorporates the external boundary layer mass transport and homogeneous diffusion inside the particle. A new orthogonal collocation method has been developed and used to solve the diffusion equations. This orthogonal collocation gives a faster solution method compared with the numerical Crank–Nicolson method. The surface diffusivity has been determined by an optimization procedure with minimization of sum of the error squared. The equilibrium relationship between the liquid-phase concentration and the solid-phase concentration has been described by the Redlich–Peterson isotherm. A solid-phase concentration-dependent surface diffusivity was introduced. The Darken model with the Redlich–Peterson isotherm was found to be a suitable correlation model for the adsorption of the acid dyes on carbon. The magnitude of the averaged D_{s0} of each dye is in the order of AR114 > AB80 > AY117, which implies that, under the same solid-phase concentration gradient, the rate of mass transport diffusion is higher in AR114 than that in AB80 and AY117. This phenomenon may be explained by the different mobilities of the dye molecules present in the solution by the different arrangements of two sulfonic acid groups in the dye structures. *AIChE J,* 51: 323–332, 2005
Keywords: surface diffusion model, orthogonal collocation, adsorption, acid dyes, activated carbon

Introduction

Activated carbons are known to have extremely large surface areas.[1] In addition, the adsorption capacity of acid dyes on activated carbon is relatively higher than that of several other adsorbents.[2] Fixed-bed adsorption is an effective contacting operation that can provide a high degree of pollutant removal from effluents in a continuous adsorption system.

The rate of mass transfer of the adsorbate is the reason for this phenomenon. The mechanism of solute adsorption onto an adsorbent can be described by three steps:

(1) Mass transfer of solute from the bulk solution through the stagnant film surroundings to the particle external surface (external film mass transfer).

(2) Mass transfer of solute within the particle (internal mass transfer).

(3) Solute attached onto the surface of the adsorbent surface site (adsorption).

One or more of these three steps may be involved in the mass transfer rate controlling step. Mathews and Weber[3] developed a solid-phase, homogeneous surface diffusion model (HSDM),

Correspondence concerning this article should be addressed to G. McKay at

using the finite-difference solution method for any arbitrary isotherm in a batch-adsorption system. The HSDM has been successfully extended to fixed-bed adsorption systems on activated carbon.[4-8]

The variation of surface diffusivities resulting from the change of solid-phase concentration has been investigated for a long time. There were three main types of justification presented in the literature. The first one is the increase of the hopping distance with an increase of the solid-phase concentration in a surface hopping model.[9] The second explanation is the change of the ratio of the chemical potential gradient to the gradient of the amount adsorbed with an increase of the solid-phase concentration. The third explanation is the decrease of the heat of adsorption with an increase of the solid-phase concentration.[10] Although the work of Neretnieks[10] focused on a pore-surface diffusion mechanism, the phenomenon of the variation of surface diffusivities was explained by using a strongly nonlinear isotherm, such as the Temkin isotherm, which is based on the assumption that the heat of adsorption decreases linearly with an increase of concentration. However, there was no detailed explanation of the variation.

The hopping of molecules is a mechanical model developed by Higashi et al.,[9] although it is applicable only to a monolayer adsorption system. Yang et al.[11] modified the work of Higashi et al. for multilayer adsorption systems. However, Suzuki[12] pointed out that the hopping of adsorbed molecules is less likely in the aqueous phase than in the gaseous phase because the energy accompanied with the molecules is high in the gaseous phase.

Based on the change of the chemical potential gradient arising from the change of the solid-phase concentration, the relationship between the surface diffusivities and the solid-phase concentration was developed by using equilibrium isotherm models.[13] It is applicable to all equilibrium isotherms, except for the Freundlich isotherm equation, because the derivative term inside this model is independent of the solid-phase concentration when the Freundlich isotherm equation is used.[12]

Several expressions were then developed based on the decrease of heat of adsorption with an increase of the solid-phase concentration.[12,14] These expressions are applicable to liquid-phase adsorption systems, but they were developed for batch-adsorption systems. These proposed models used the amount of substrate adsorbed on the adsorbent as the variable. It is difficult in a fixed-bed system to calculate the final equilibrium amount adsorbed.[15] The final equilibrium amount adsorbed is different along the bed. Thus, the application of the equilibrium solid-phase concentration was used in a model developed by Muraki et al.[15] However, all these models, based on the decrease in the heat of adsorption, were developed with the Freundlich isotherm equation.

This study applies the orthogonal collocation solution method to the acid dye fixed-bed adsorption systems on activated carbon. This orthogonal collocation gives a faster solution method compared with the earlier, numerical Crank–Nicolson method.[16] The surface diffusivities of the adsorption systems under different operating conditions, such as liquid volumetric flow rate, initial dye concentration, and particle size range, are determined in this study.

Mathematical Model

The basis of this model was proposed by Mathews and Weber[3] and included the effect of external mass transfer, unsteady-state surface diffusion in the particle, and a nonlinear adsorption isotherm. The mechanistic processes that are considered in representing single-component adsorption are based on the diffusion of an adsorbate through an external film to the outer surface of a particle. Once reaching the surface, adsorption occurs instantaneously and equilibrium is assumed to be established between the adsorbate fluid and that on the surface. The assumptions of HSDM are as follows:

(1) The adsorbent particle [granular activated carbon (GAC)] is assumed to be a homogeneous solid sphere in which the adsorbate is transported by surface diffusion.

(2) The rate-controlling processes are mass transport based on film and surface diffusion model only.

(3) A driving force describes the liquid film transport resistance at the outer surface of the particle.

The basic equations for the mathematical model of HSDM are described in the following section and are based on models developed by previous researchers.[3,4,17]

The mathematical model was developed starting by the overall mass balance around the fixed bed. This was governed by the following equation

$$\frac{\partial C_t}{\partial t} + u\,\frac{\partial C_t}{\partial z} + \rho_p\,\frac{1-\varepsilon}{\varepsilon}\,\frac{\partial q_t}{\partial t} = 0 \tag{1}$$

The third term represents the rate of mass transport diffusion into the particle. The adsorbate molecules first diffuse across the stagnant liquid film. This mass transport can be represented by the following equation

$$\rho_p\,\frac{\partial q_t}{\partial t} = \frac{3k_f(C_t - C_s)}{R} \tag{2}$$

To generate a general solution, it is better to represent the mass transport model in a dimensionless form. Introducing the following dimensional and dimensionless terms

$$\xi = \frac{C_t}{C_0} \tag{3}$$

$$\eta_t = \frac{q_t}{q_e} \tag{4}$$

$$\bar{t} = \frac{t}{\tau_s D_g} \tag{5}$$

$$D_g = \frac{\rho_p q_e(1-\varepsilon)}{C_0\varepsilon} \tag{6}$$

$$\mathrm{Sh}_{HSDM} = \frac{k_f(1-\varepsilon)\tau_s}{\varepsilon R} \tag{7}$$

where

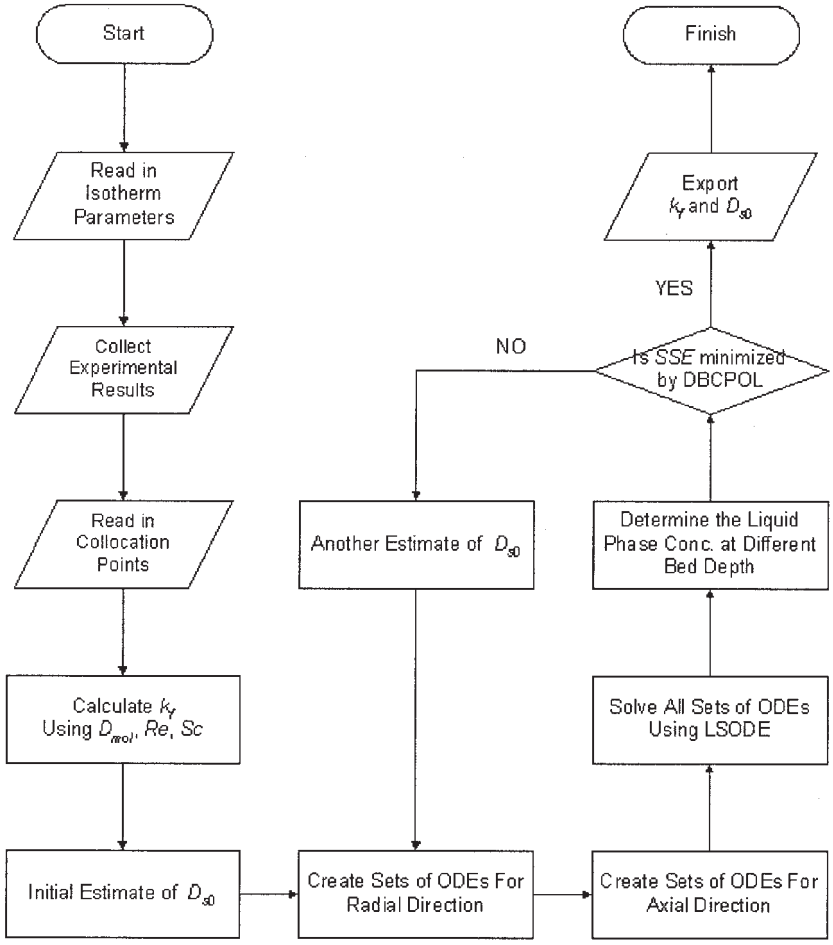

Figure 1. Algorithm for solving HSDM.

$$\tau_s = \frac{L}{u} \tag{8}$$

Equation 2 becomes a dimensionless equation, which is

$$\frac{\partial \eta_t}{\partial \bar{t}} = 3\mathrm{Sh}_{HSDM}(\xi - \xi_s) \tag{9}$$

In addition, by substituting Eq. 2 into Eq. 1, the mass balance around the fixed bed becomes

$$\frac{\partial C_t}{\partial t} + u\frac{\partial C}{\partial z} + \frac{3k_f(1-\varepsilon)}{\varepsilon R}(C_t - C_s) = 0 \tag{10}$$

The initial and boundary conditions of this mass balance equation are

$$C_t(z, 0) = 0 \tag{11}$$

$$C_t(0, t) = C_0 \tag{12}$$

Equation 11 represents that the initial liquid-phase concentration of the column is equal to zero for all bed heights. Equation 12 implies that the liquid-phase concentration of influents at zero bed heights throughout the experiment is C_0 (that is, a step change of the input concentration). Replacing Eq. 10 with dimensionless terms shown in Eqs. 3 to 7 and the following dimensionless bed depth term

$$\bar{z} = \frac{z}{L} \tag{13}$$

Equation 10 becomes a dimensionless form, which is

$$\frac{1}{D_g}\frac{\partial \xi}{\partial \bar{t}} + \frac{\partial \xi}{\partial \bar{z}} + 3\mathrm{Sh}_{HSDM}(\xi - \xi_s) = 0 \tag{14}$$

The transformed initial and boundary conditions in dimensionless form are

$$\xi(\bar{z}, 0) = 0 \tag{15}$$

$$\xi(0, \bar{t}) = 1 \tag{16}$$

After considering the mass balance across the bed, the mass transport diffusion inside the particle is evaluated. It is assumed

that surface diffusion is the rate-determining step of the mass transport diffusion inside the particle. The mathematical expressions representing the rate of diffusion are

$$\frac{\partial q_t}{\partial t} = \nabla \cdot (D_s \nabla q_t) \tag{17}$$

$$\frac{\partial q_t}{\partial t} = \frac{1}{r^2}\left[D_s \frac{\partial}{\partial r}\left(r^2 \frac{\partial q_t}{\partial r}\right) + r^2 \frac{\partial q_t}{\partial r}\frac{\partial D_s}{\partial r}\right] \tag{18}$$

The change of D_s is less significant than that of q_t with respect to r. Thus, the last term of Eq. 18 is neglected. Therefore, Eq. 18 becomes

$$\frac{\partial q_t}{\partial t} = \frac{D_s}{r^2}\frac{\partial}{\partial r}\left(r^2 \frac{\partial q_t}{\partial r}\right) \tag{19}$$

The initial and boundary conditions of the above equation are

$$q_t(r, 0) = 0 \tag{20}$$

$$q_t(R, t) = q_s(t) \tag{21}$$

$$\frac{\partial q_t}{\partial r}(0, t) = 0 \tag{22}$$

The initial solid-phase concentration at the whole adsorbent particle equals zero and is represented by Eq. 20. The solid-phase concentration at the outer surface is at equilibrium with the liquid-phase concentration, which was previously calculated in the film mass transport, and is represented by Eq. 21. It is assumed that the particle is symmetrical around the center of the particle. Therefore, the rate of change of solid-phase concentration with respect to the radius of the particle across the center is zero, which is represented by Eq. 22. Introducing the following dimensional and dimensionless terms

$$\bar{r} = \frac{r}{R} \tag{23}$$

$$N_d = \frac{D_s D_g \tau_s}{R^2} \tag{24}$$

The homogeneous diffusion equation (Eq. 19) becomes

$$\frac{\partial \eta_t}{\partial \bar{t}} = \frac{N_d}{\bar{r}^2}\frac{\partial}{\partial \bar{r}}\left(\bar{r}^2 \frac{\partial \eta_t}{\partial \bar{r}}\right) \tag{25}$$

with the following transformed dimensionless initial and boundary conditions

$$\eta_t(\bar{r}, 0) = 0 \tag{26}$$

$$\eta_t(1, \bar{t}) = \eta_s \tag{27}$$

$$\frac{\partial \eta_t}{\partial \bar{r}}(0, \bar{t}) = 0 \tag{28}$$

The Redlich–Peterson isotherm,[18] used to describe the adsorption equilibrium at the interface of solid and liquid, was found to be the most suitable isotherm to describe the acid dye/activated carbon adsorption system.[19] The Redlich–Peterson isotherm is expressed as follows

$$q_s = \frac{K_R C_s}{1 + a_R C_s^{\beta_R}} \tag{29}$$

Darken[13] defined a relationship between the diffusivities and chemical potentials. The surface diffusion flux J_s is related to the chemical potential gradient with respected to concentration by

$$J_s = -L_p q_t^* \frac{d\mu}{dx} \tag{30}$$

The chemical potential related to the reference chemical potential μ_0, at equilibrium condition, is given by

$$\mu = \mu_0 + R'T \ln C_t^* \tag{31}$$

where μ_0 is the reference chemical potential.

Equation 31 was substituted into Eq. 30, yielding

$$J_s = -D_{s0} q_t^* \frac{d \ln C_t^*}{dx} \tag{32}$$

where $D_{s0} = L_p R'T$.

Given that

$$J_s = -D_s \frac{dq_t^*}{dx} \tag{33}$$

thus, by comparing Eq. 32 and Eq. 33, a correlation of D_{s0} becomes

$$D_s = D_{s0} \frac{\partial \ln C_t^*}{\partial \ln q_t^*} \tag{34}$$

The derivative term of Eq. 34 can be determined by incorporating the appropriate isotherm equation.

In the present work, the Redlich–Peterson isotherm equation has been used to describe acid dye–carbon equilibrium; this approach has not been applied in a variable diffusivity solution before. By the chain rule, the differential component in Eq. 34 can be expanded, that is

$$\frac{\partial \ln C_t^*}{\partial \ln q_t^*} = \frac{\partial \ln C_t^*}{\partial C_t^*}\frac{\partial C_t^*}{\partial q_t^*}\frac{\partial q_t^*}{\partial \ln q_t^*} \tag{35}$$

Simplifying Eq. 35 yields the following equation:

Table 1. Details of Acid Dyes

Name of Dyes	Abbreviation	Manufacturer	λ_{max} (nm)
Acid Blue 80	AB80	Ciba Specialty Chemicals (Hong Kong)	626
Acid Red 114	AR114	Aldrich (St. Louis, MO)	522
Acid Yellow 117	AY117	Ciba Specialty Chemicals (Hong Kong)	438

$$\frac{\partial \ln C_t^*}{\partial \ln q_t^*} = \frac{q_t^*}{C_t^*}\frac{\partial C_t^*}{\partial q_t^*} \tag{36}$$

A modified Redlich–Peterson isotherm equation is used to describe the equilibrium concentrations at the solid phase and the liquid phase. The equation is defined as

$$q_t^* = RP(C_t^*) = \frac{\rho_p\left(\frac{1}{1-\varepsilon}\right)K_R C_t^*}{1 + a_R C_t^{*\beta_R}} \tag{37}$$

Equation 37 is defined as

$$q_t^* = \frac{K_R^* C_t^*}{1 + a_R C_t^{*\beta_R}} \tag{38}$$

and thus by rearranging Eq. 38, we obtain

$$C_t^* = RP^{-1}(q_t^*) \tag{39}$$

Differentiating Eq. 38, with respect to C_t^*, yields

$$\frac{\partial q_t^*}{\partial C_t^*} = \frac{K_R^*[1 + a_R C_t^{*\beta_R}(1-\beta_R)]}{(1 + a_R C_t^{*\beta_R})^2} \tag{40}$$

given that

$$\frac{\partial C_t^*}{\partial q_t^*} = \frac{1}{\frac{\partial q_t^*}{\partial C_t^*}} \tag{41}$$

$$\frac{\partial C_t^*}{\partial q_t^*} = \frac{(1 + a_R C_t^{*\beta_R})^2}{K_R^*[1 + a_R C_t^{*\beta_R}(1-\beta_R)]} \tag{42}$$

Equations 38 and 42 are substituted into Eq. 36, as shown

$$\frac{\partial \ln C_t^*}{\partial \ln q_t^*} = \frac{1 + a_R C_t^{*\beta_R}}{1 + a_R C_t^{*\beta_R}(1-\beta_R)} \tag{43}$$

Equation 39 is substituted into Eq. 43 to give

$$\frac{\partial \ln C_t^*}{\partial \ln q_t^*} = \frac{1 + a_R[RP^{-1}(q_t^*)]^{\beta_R}}{1 + a_R[RP^{-1}(q_t^*)]^{\beta_R}(1-\beta_R)} \tag{44}$$

The derivative term of Eq. 34 can be replaced by Eq. 44 and we obtain

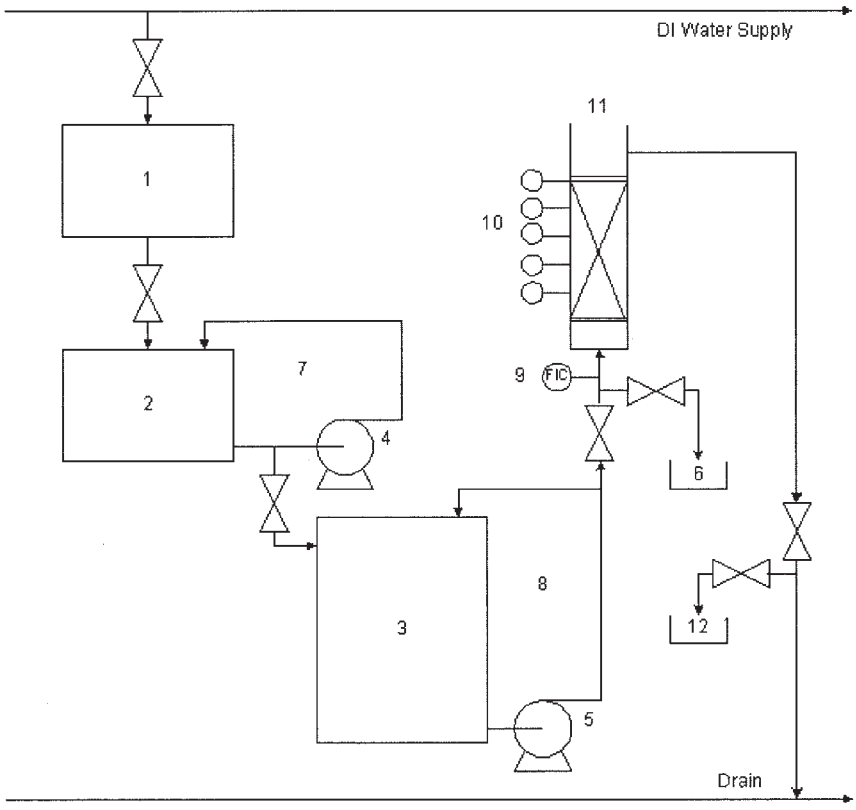

Figure 2. Experimental system for fixed-bed operation.

Table 2. Equipment Specification for Adsorption Column Pilot Plant

Item Number	Description	Specification
1	50 dm^3 plastic container	
2	50 dm^3 plastic containers with recirculation agitation	
3	100 dm^3 plastic containers with recirculation agitation	
4 and 5	Centrifugal pump 1/6 hp ac motors	
6	Sampling points to check on initial influent concentration	
7 and 8	Three-way valves	
9	Rotameter	
10	Sampling points Subar seals for syringes (10 cm^3)	
11	Perspex columns	ID = 0.045 m Length = 0.25 m

$$D_s = D_{s0}\frac{1 + a_R[RP^{-1}(q_t^*)]^{\beta_R}}{1 + a_R[RP^{-1}(q_t^*)]^{\beta_R}(1 - \beta_R)} \tag{45}$$

Equation 45 shows the relationship between D_s and the adsorbed-phase concentration using the Darken relationship.

A solution method, developed to solve the model equations, was solved using the orthogonal collocation procedure described by Finlayson.[20] It has been used to solve the mathematical models in some adsorption systems.[21,22] By changing the operating parameters of the fixed bed studies, such as flow rate and initial concentration, the effect of these operating parameters on each mass-transfer parameter will be found in this research. The algorithm of the solution development is shown in Figure 1. A system of ordinary differential equations of mass transfer equations in radial and axial directions was generated from Eqs. 14 and 25 using the orthogonal collocation method. A computational program of the solution is written in Fortran 77. The system of ordinary differential equations at the collocation points is solved by a program subroutine LSODE.[23] The sum of squares of the error (SSE) is defined as

$$\mathrm{SSE}_t = \frac{1}{n}\sum_{i=1}^{n}(C_{\exp} - C_{\mathrm{cal}})_i^2 \tag{46}$$

where C_{exp} is the experimental liquid-phase concentration and C_{cal} is the calculated liquid-phase concentration. Using a built-in function DBCPOL, supplied by the IMSL library, this sum of squares of the error is minimized by varying the model parameters.

Experimental

Materials

The adsorbent used in this study is Filtrasorb 400 granular activated carbon (GAC) supplied by Chemviron Ltd. The GAC was washed in deionized water, dried, and sieved to obtain certain size ranges: 355–500, 500–710, and 710–1000 μm. The particles are assumed to be spheres having a diameter given by the arithmetic mean value between respective mesh sizes (that is, 427.5, 605, and 855 μm). The available surface for Filtrasorb 400 was found to be 1150 m^2/g by nitrogen adsorption using a BET analysis. The physical properties of the GAC were determined by the Micromeritics® Poresizer 9320. The void fraction and particle density of the particle are 0.38 and 1300 kg/m^3, respectively. The dyestuffs used as the adsorbates are Polar Blue RAWL (Acid Blue 80, AB80), Acid Red 114 (AR114), and Polar Yellow (Acid Yellow 117, AY117). The concentration of dyestuffs was measured by a Varian Cary 1E UV–vis spectrophotometer at specific wavelengths for each dyestuff at which maximum absorption of light occurs, λ_{max}. The details for each dyestuff are listed in Table 1.

Procedures

A schematic of the fixed-bed pilot plant apparatus is shown in Figure 2. The deionized water used was from a central supply and was fed into a 50-dm^3 plastic container as listed in Table 2 (Item 1). A known amount of dye salt was added to

Table 3. Summary of HSDM Parameters with Variable Surface Diffusivity (Optimized in Each Operating Condition)

Dye	C_0 (g/m^3)	F (cm^3/min)	d_p (μm)	$k_f \times 10^6$ (m/s)	$D_{s0} \times 10^{15}$ (m^2/s)	SSE
AB80	100	30	605	1.49	1.48	1.27×10^{-3}
	100	40	605	1.65	1.41	9.43×10^{-4}
	100	60	605	1.90	2.00	1.24×10^{-3}
	100	80	605	2.10	2.07	1.05×10^{-3}
	50	30	605	1.49	0.82	5.68×10^{-3}
	100	30	605	1.49	1.48	1.27×10^{-3}
	150	30	605	1.49	2.02	4.32×10^{-3}
	50	30	427.5	2.39	0.80	3.40×10^{-3}
	50	30	605	1.49	0.82	5.68×10^{-3}
	50	30	855	0.94	0.91	3.82×10^{-3}
AR114	100	30	605	1.32	4.18	1.25×10^{-3}
	100	40	605	1.46	4.42	2.56×10^{-3}
	100	60	605	1.68	4.91	2.17×10^{-3}
	100	80	605	1.86	4.99	1.69×10^{-3}
AY117	100	30	605	1.29	1.39	2.62×10^{-3}
	100	40	605	1.43	1.15	4.92×10^{-3}
	100	60	605	1.64	1.59	2.55×10^{-3}
	100	80	605	1.82	1.94	1.66×10^{-3}
	50	40	605	1.43	0.84	6.51×10^{-3}
	100	40	605	1.43	1.15	4.92×10^{-3}
	150	40	605	1.43	1.37	4.00×10^{-3}

Table 4. Summary of HSDM Parameters with Variable Surface Diffusivity (Using a Fixed D_{s0} for Each Dye)

Dye	C_0 (g/m^3)	F (cm^3/min)	d_p (μm)	$k_f \times 10^6$ (m/s)	$D_{s0} \times 10^{15}$ (m^2/s)	SSE
AB80	100	30	605	1.49	1.50	1.28×10^{-3}
	100	40	605	1.65	1.50	1.18×10^{-3}
	100	60	605	1.90	1.50	5.29×10^{-3}
	100	80	605	2.10	1.50	4.54×10^{-3}
	50	30	605	1.49	1.50	3.32×10^{-2}
	100	30	605	1.49	1.50	1.28×10^{-3}
	150	30	605	1.49	1.50	1.20×10^{-2}
	50	30	427.5	2.39	1.50	1.88×10^{-2}
	50	30	605	1.49	1.50	3.32×10^{-2}
	50	30	855	0.94	1.50	2.13×10^{-2}
AR114	100	30	605	1.32	4.63	1.82×10^{-3}
	100	40	605	1.46	4.63	2.63×10^{-3}
	100	60	605	1.68	4.63	2.29×10^{-3}
	100	80	605	1.86	4.63	1.87×10^{-3}
AY117	100	30	605	1.29	1.35	2.65×10^{-3}
	100	40	605	1.43	1.35	6.05×10^{-3}
	100	60	605	1.64	1.35	3.31×10^{-3}
	100	80	605	1.82	1.35	5.24×10^{-3}
	50	40	605	1.43	1.35	3.02×10^{-2}
	100	30	605	1.29	1.35	6.05×10^{-3}
	150	40	605	1.43	1.35	4.01×10^{-3}

another plastic container (Item 2) with a batch of 50 dm^3 of water from Item 1 and this solution was mixed by recirculation. The solution was then transferred into another similar tank (Item 3). Samples were taken from a sampling point (Item 6) to record the value of the initial concentration used in each test run. Influent to the adsorption beds was pumped by a centrifugal pump (Item 5). A three-way valve (Item 8) served to control the recycle feedback to the constant head tank (Item 3). Calibrated rotameters (Item 9) were used to control the flow rate through the columns (Item 11). Finally, the effluent was discharged into a drain.

Sample points were located at various heights (Item 10) 0.05 m apart, on the adsorbent column (Item 11), and 10 cm^3 syringes and stainless steel needles were used to obtain sample solutions from the adsorption beds. The samples were analyzed using a Varian Cary 1E UV spectrophotometer.

Model Application and Discussion

The methodology involving the Redlich–Peterson isotherm was developed in the previous section. The values of the parameters of the Redlich–Peterson isotherm were previously determined by Choy et al.[19] The remaining variable of the solution system is D_{s0}. Table 3 shows the optimized D_{s0} for each operating condition for the acid dyes adsorption using the HSDM with a variable surface diffusivity. The D_{s0} is the surface diffusivity at zero surface loading. Thus, theoretically, the value D_{s0} is dependent solely on the dye characteristic. It is assumed that this constant value of D_{s0} is the average value of surface diffusivity determined for each operating condition of each dye. The sum of the squares of the error was then calculated again using these constant rationalized values of D_{s0} for each dye and the results are shown in Table 4.

The magnitude of the averaged D_{s0} of each dye is in the order of AR114 > AB80 > AY117, which is identical to the order of surface diffusivity D_s, if using a fixed surface diffusivity instead of a variable one. This implies that, under the same solid-phase concentration gradient, the rate of mass transport diffusion is higher in AR114 than that in AB80 and AY117, which is the surface diffusivity at zero loading. There are two sulfonic acid groups in the dye structure of each dye. However, locations of these two sulfonic acid groups are quite different. The sulfonic acid groups are attached at the same benzene ring in the AR114 molecular structure (as shown in Figure 3), whereas the sulfonic acid groups are attached at the two opposite ends of the dye molecule in AB80 and AY117. The surface mobility of AR114 molecules may be higher than that of AB80 and AY117 because of the arrangement of sulfonic acid groups in the AR114 molecule. Therefore, the determined surface diffusivity at zero surface loading of AR114 is the highest.

In the study of the volumetric flow rate effect, the change of the sum of the squares of the error by using a constant D_{s0} is not significant compared with using an optimized D_{s0}. There is

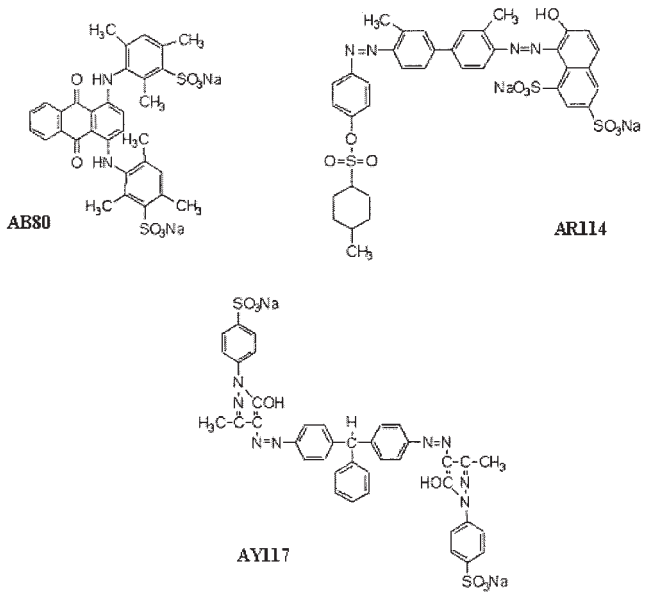

Figure 3. Dye structures of acid dyes.

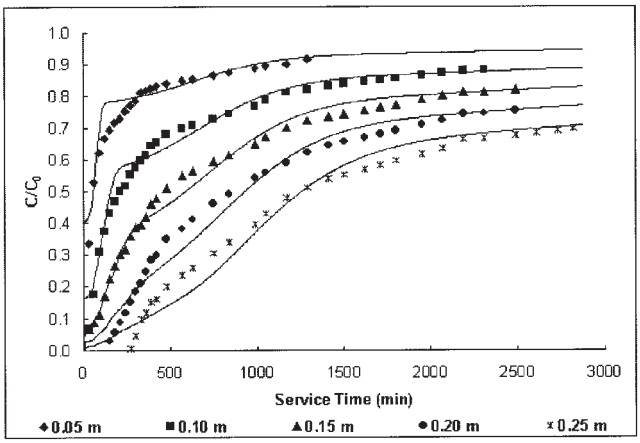

Figure 4. Example of HSDM using variable surface diffusivity.

Dye = AB80, $F = 30\ \text{cm}^3/\text{min}$, $C_0 = 100\ \text{g/m}^3$, $d_p = 655\ \mu\text{m}$.

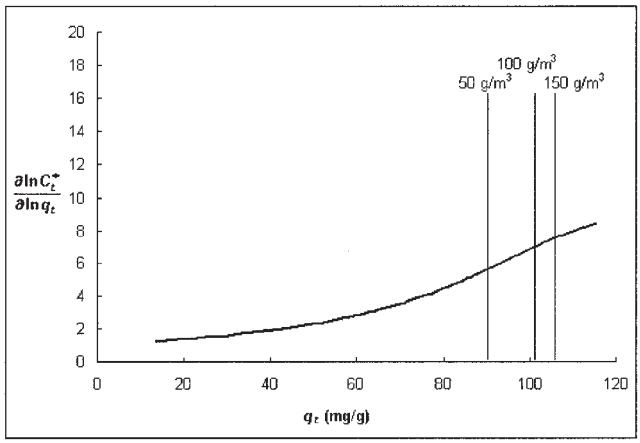

Figure 6. Variation of Darken expression with the change of solid-phase concentration (AR114).

only a slight discrepancy in the results with high flow rate because a high flow rate is more difficult to control during the experiments, which may account for the discrepancy.

An example of the HSDM using a variable surface diffusivity is shown in Figure 4. There is a noticeable change of the breakthrough curve using a variable surface diffusivity. A large surface diffusivity enhances the mass transport of the adsorbate inside the particle, and thus a large surface diffusivity results in a flatter breakthrough curve. Because there is an increase of surface diffusivity with an increase of time as the result of an increase of surface loading, a concave-like shape curve occurs in the breakthrough curve as a consequence of the changing surface diffusivity.

The methodology developed in this research project can be used for different isotherms, and thus the results from different isotherm were analyzed. Figures 5 to 7 show the variation of the Darken expression with the change of the solid-phase concentration using different isotherm equations in AB80, AR114, and AY117 adsorption systems, respectively. The figures imply that the Darken expression is sensitive to the choice of the isotherm equations. Given that the Redlich–Peterson isotherm was found to be the most suitable isotherm for describing the adsorption of acid dyes on activated carbon,[19] the analysis of this research project was based on the Redlich–Peterson isotherm.

Results of the HSDM, using fixed-surface diffusivity and variable-surface diffusivity, can be compared in Table 5, which shows the averaged sum of the squares of the errors for the acid dyes in the HSDM using both fixed- and variable-surface diffusivities.

A noticeable improvement was seen only for AR114 when using a variable-surface diffusivity instead of using fixed-surface diffusivity. The average surface coverage of AR114 was 0.23, whereas values for AB80 and AY117 were 0.18 and 0.19, respectively. Thus, the average surface coverage of AR114 is slightly higher than that of AB80 and AY117. Higashi et al.[9] proposed a hopping model. The surface diffusion is explained by the jumping of molecules adsorbed in one site to other vacant sites. If the sites are occupied, then the molecules continue to jump until they find vacant sites. The number of hopping phenomena necessary to find vacant sites is increased when the average surface coverage is increased. Because a high solid-phase concentration results in a large

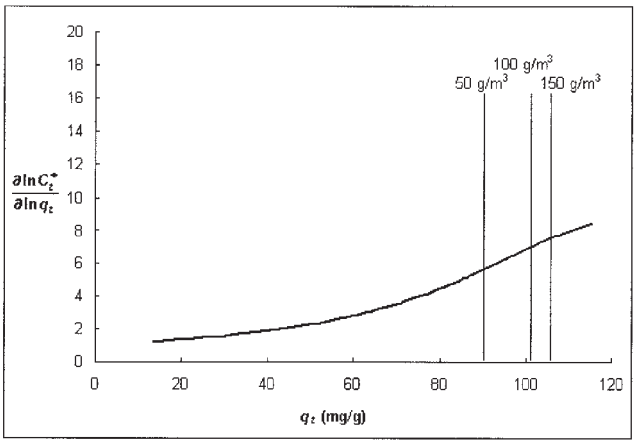

Figure 5. Variation of Darken expression with the change of solid-phase concentration (AB80).

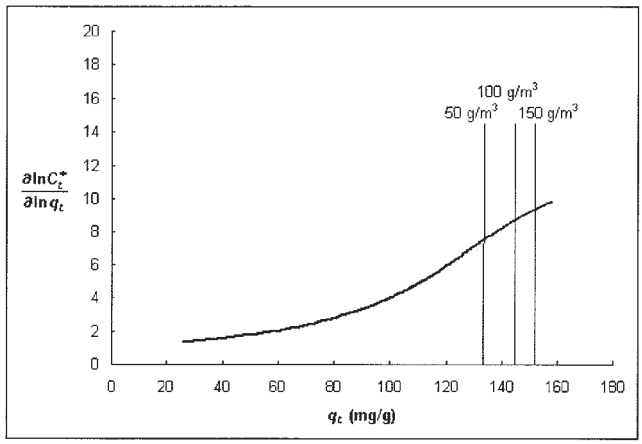

Figure 7. Variation of Darken expression with the change of solid-phase concentration (AY117).

Table 5. Comparison of SSE in HSDM Using Fixed-Surface Diffusivity and Variable-Surface Diffusivity

Dye	Average SSE	
	Using Fixed-Surface Diffusivity	Using Variable-Surface Diffusivity
AB80	1.28×10^{-2}	1.22×10^{-2}
AR114	2.56×10^{-3}	2.15×10^{-3}
AY117	7.51×10^{-3}	8.59×10^{-3}

average surface coverage, a high solid-phase concentration results in a large surface diffusivity. Figure 6 shows that the change of surface diffusivity (the slope of the graph) is high at a high solid-phase concentration, and thus the change of surface diffusivity is significant at a high solid-phase concentration. A noticeable improvement was seen only for AR114 when using a variable-surface diffusivity instead of using fixed-surface diffusivity.

Conclusion

An orthogonal collocation solution method was developed in this research. It was found that the Darken model[13] with the Redlich–Peterson isotherm was a suitable surface diffusivity correlation for the current research. The derivative term in the Darken model, involving the Redlich–Peterson isotherm, could not be solved analytically. Thus, a numerical method was developed. The averaged surface diffusivities at zero surface loadings of AB80, AR114, and AY117 were determined as 1.50×10^{-15}, 4.63×10^{-15}, and 1.35×10^{-15} m/s, respectively. The magnitude of the averaged D_{s0} of each dye is related to the location of these two sulfonic acid groups in the acid dye molecular structures. Different locations of these two sulfonic acid groups induce different surface mobilities of dye molecules. Thus, the surface mobility of AR114 molecules may be higher than that of AB80 and AY117 because of the arrangement of sulfonic acid groups in the AR114 molecule. The results of the HSDM using fixed-surface diffusivity and variable-surface diffusivity were compared. A noticeable improvement was seen for only AR114 when using a variable-surface diffusivity instead of using fixed-surface diffusivity, which may be explained by different average surface coverage in AR114 compared with that of AB80 and AY117.

Acknowledgments

The authors thank the Research Grant Council (RGC) for providing support for this research.

Notation

a_R = Redlich–Peterson isotherm parameter, $(m^3/g)^{\beta R}$
C_0 = initial dye concentration, g/m^3
C_{cal} = calculated liquid-phase concentration, g/m^3
C_{exp} = experimental liquid-phase concentration, g/m^3
C_s = liquid-phase concentration at adsorbent external surface, g/m^3
C_t = liquid-phase concentration at time t, g/m^3
C_t^* = equilibrium liquid-phase concentration at time t with respect to q_t^*, g/m^3
D_g = partition coefficient defined in Eq. 6, dimensionless
d_p = mean particle size, μm
D_s = surface diffusivity, m^2/s
D_{s0} = surface diffusivity at zero surface loading, m^2/s
F = volumetric flow rate, cm^3/min
J_s = surface diffusion flux, $g/m^{2}\cdot s$
k_f = external mass transfer coefficient, m/s
K_R = Redlich–Peterson isotherm parameter, m^3/g
K_R^* = modified Redlich–Peterson isotherm parameter, g/g
L = length of the bed, m
L_p = length of the porous medium, m
N_d = dimensionless surface diffusivity
q_e = equilibrium solid-phase concentration, g/g
q_s = solid-phase concentration at the surface of adsorbent, g/g
q_t = solid-phase concentration at time t, g/g
q_t^* = solid-phase concentration at time t, g/m^3
R = radial dimension of particle, m
$\bar{r}$ = dimensionless radial dimension of particle
R = radius of adsorbent particle, m
R' = gas constant, J mol^{-1} K^{-1}
RP = function of Redlich–Peterson isotherm, g/m^3
Sh_{HSDM} = Sherwood number defined for HSDM, dimensionless
t = service time of the bed, s
$\bar{t}$ = dimensionless service time of the bed
T = temperature, K
u = linear fluid velocity, m/s
x = coordinate along the direction of mass transfer, m
z = bed height, m
$\bar{z}$ = dimensionless bed height

Greek letters

β_R = Redlich–Peterson isotherm parameter, dimensionless
ε = void fraction, dimensionless
η_s = dimensionless solid-phase concentration at the outer surface of the particle
η_t = dimensionless solid-phase concentration at time t
λ_{max} = wavelength at maximum absorption of light, nm
μ = chemical potential, J/mol
μ_0 = reference chemical potential, J/mol
ξ = dimensionless liquid-phase concentration
ξ_s = dimensionless liquid-phase concentration at adsorbent external surface
ρ_p = particle density, g/m^3
τ_s = nonempty bed residence time, s

Literature Cited

1. McKay G. The adsorption of dyestuffs from aqueous solutions using activated carbon: Analytical solution for batch adsorption based on external mass transfer and pore diffusion. *Chemical Engineering Journal.* 1983;27:187-196.
2. Choy KH. *Modelling the Diffusion of Acid Dyes on Activated Carbon*. PhD Dissertation. Hong Kong SAR, China: The Hong Kong University of Science and Technology; 2001.
3. Mathews AP, Weber WJJ. Effects of external mass transfer and intraparticle diffusion on adsorption rates in slurry reactors. *AIChE Symposium Series.* 1976;73:91-107.
4. Crittenden JC, Weber WJJ. Predictive model for design of fixed-bed adsorbers: Parameter estimation and model development. *Journal of Environmental Engineering.* 1978;104:185-197.
5. Olmstead KP, Weber WJJ. Statistical analysis of mass-transfer parameters for sorption processes and models. *Environmental Science & Technology.* 1990;24:1693-1700.
6. Slaney AJ, Bhamidimarri R. Adsorption of pentachlorophenol (PCP) by activated carbon in fixed beds: Application of homogeneous surface diffusion model. *Water Science and Technology.* 1998;38:227-235.
7. Pota AA, Mathews AP. Effects of particle stratification on fixed bed absorber performance. *Journal of Environmental Engineering.* 1999; 125:705-711.
8. Pota AA, Mathews AP. Adsorption dynamics in a stratified convergent tapered bed. *Chemical Engineering Science.* 2000;55:1399-1409.
9. Higashi K, Ito H, Oishi J. Surface diffusion phenomena in gaseous diffusion: I. Surface diffusion of pure gas. *Journal of the Atomic Energy Society of Japan.* 1963;5:846-853.
10. Neretnieks I. Analysis of some adsorption experiments with activated carbon. *Chemical Engineering Science.* 1976;31:1029-1035.
11. Yang RT, Fenn JB, Haller G. Modification to the Higashi model for surface diffusion. *AIChE Journal.* 1973;19:1052-1053.
12. Suzuki M. Concentration dependence of effective surface diffusion

coefficients in aqueous phase adsorption on activated carbon. *Chemical Engineering Science.* 1978;33:1287-1290.
13. Darken LS. Diffusion, mobility and their interrelation through free energy in binary metallic systems. *Transactions of the American Institute of Mining Engineers.* 1948;175:184.
14. Suzuki M, Fujii T. Concentration dependence of surface diffusion coefficient of propionic acid in activated carbon particles. *AIChE Journal.* 1982;28:382-385.
15. Muraki M, Iwashima Y, Hayakawa T. Rate of liquid-phase adsorption on activated carbon in the stirred tank. *Journal of Chemical Engineering of Japan.* 1982;15:34-39.
16. Crank J. *The Mathematics of Diffusion*. 1st ed. Oxford, UK: Clarendon Press; 1947.
17. Thacker WE, Snoeyink V, Crittenden JC. Modeling of activated carbon and coal gasification char adsorbents in single solute and biosolute. Research Report No. 161. Urbana, IL: Water Research Center, University of Illinois; 1981.
18. Redlich O, Peterson, DL. A useful adsorption isotherm. *Journal of Physical Chemistry.* 1959;63:1024.
19. Choy KKH, Porter JP, McKay G. Sorption of acid dyes from effluents using activated carbon. *Resources Conservation and Recycling.* 1999; 27:57-71.
20. Finlayson BA. *The Method of Weighted Residuals and Variational Principles, with Application in Fluid Mechanics, Heat, and Mass Transfer*. 1st ed. New York, NY: Academic Press; 1972.
21. Tien C. *Adsorption Calculations and Modeling*. 1st ed. Boston, MA: Butterworth-Heinemann; 1994.
22. Do DD. *Adsorption Analysis: Equilibria and Kinetics*. 1st ed. London: Imperial College Press; 1998.
23. Hindmarsh AC. LSODE and LSOD1: Two new initial value ordinary differential equation solvers. *ACM-SIGNUM Newsletter.* 1980;15:10-11.

Manuscript received Aug. 9, 2003, and revision received May 5, 2004.